J. Phys. Chem. A **2009,** *113,* 13921–13931

Predictions of the Fluorine NMR Chemical Shifts of Perfluorinated Carboxylic Acids, $C_nF_{2n+1}COOH$ ($n = 6-8$)

Zizhong Liu[†,‡] **and John D. Goddard***[,†]

Department of Chemistry, University of Guelph, Guelph, Ontario, Canada N1G 2W1, and Chemistry and Environment Science College, Inner Mongolia Normal University, Huhhot, Inner Mongolia, China 010022

Received: August 12, 2009; Revised Manuscript Received: October 4, 2009

Perfluorinated carboxylic acids (PFCAs) are a class of persistent environmental pollutants. Commercially available PFCAs are mixtures of linear and branched isomers, possibly with impurities. Different isomers have different physical and chemical properties and toxicities. However, little is known about the properties and the finer details of the structures of the individual branched isomers. Full geometry optimizations for the linear *n*-alkane (C_6-C_{27}) PFCAs indicated that all have helical structures. The helical angle increases slightly with increasing chain length, from 16.3° in $C_6F_{13}COOH$ to 17.0° in $C_{27}F_{55}COOH$. This study predicts ^{19}F NMR parameters for 69 linear and branched isomers of the perfluoro carboxylic acids $C_6F_{13}COOH$, $C_7F_{15}COOH$, and $C_8F_{17}COOH$. B3LYP-GIAO/6-31++G(d,p)//B3LYP/6-31G(d,p) was used for the NMR calculations with analysis of the chemical shifts by the natural bond orbital method. The predictions of the ^{19}F chemical shifts revealed the differences among the CF_3, CF_2, and CF groups. In general, the absolute values for the chemical shifts for the CF_3 group are smaller than 90 ppm, for the CF larger than 160 ppm, and for the CF_2 between 110 and 130 ppm. The chemical shifts of the branched isomers are smaller in magnitude than the linear ones. The decrease is correlated with the steric hindrance of the CF_3 groups, the more hindered the CF_3, the greater the decrease in the ^{19}F chemical shifts. The predicted ^{19}F chemical shifts are similar to those for analogous perfluoro compounds with other terminal functional groups such as $-SO_3H$ or $-SO_3NH_2CH_2CH_3$.

1. Introduction

Since the electrochemical fluorination of organic compounds in liquid hydrogen fluoride was first accomplished by Simons,[1] a variety of perfluorinated carboxylic acids (PFCAs) and other perfluorinated compounds were produced in this[2−6] and other ways.[7−13] PFCAs are a class of persistent environmental pollutants. PFCAs from electrochemical fluorination contain about 70% linear and about 30% branched isomers.[14−16] PFCAs are used, for example, in breathable waterproof fabrics, biomaterials, insulators for electric wires, planar etching of fused silica, and foam fire extinguishers. The ammonium salt of perfluorooctanoic acid (PFOA) is essential in the manufacturing of fluoropolymers.[7,17] However, PFCAs such as perfluorooctanoic acid, PFOA, have recently received much attention as ubiquitous environmental contaminants.[17−19] For example, PFOA has been detected in surface water[17,20,21] in locations around the world, and the long-chain PFCAs ($C_nF_{2n+1}-COOH$, where $n = 9-15$) have been detected in some animals from circumpolar regions.[22] The monitoring[23−28] and toxicities[29−31] of PFCAs have received much recent attention. The ^{19}F nucleus has advantageous properties for experimental NMR such as 100% natural abundance and spin $^1/_2$. ^{19}F NMR spectroscopy has become more common[32,33] and is recognized as an essential tool in the elucidation of the structures of fluorine-containing compounds.[34−37] More recently, ^{19}F NMR spectroscopy has been used to study such perfluoro compounds as linear and branched perfluorooctanesulfonamide (PFOSAmide).[14,38−41] The products of electrochemical perfluorination of *n*-alkanes (C_6-C_{10}), PFCAs, including all straight-chain and a few branched members were identified using ^{19}F NMR by Ilayaraja and co-workers.[42] No conclusions were reached from the ^{19}F NMR studies on how to best distinguish the many other isomers. The investigation of many perfluorinated carboxylic acids has not yet extended beyond the straight-chain isomers. Thus, the numerous branched congeners in different PFCAs are a poorly understood family of environmental contaminants. Their environmental, bioaccumulation, and toxicological properties may be different from those of the more prevalent straight-chain members.[15] Branched PFOS congeners, for example, have been reported to have higher aqueous solubilities than the linear isomers.[43] The branched isomers are significantly more thermodynamically stable than the linear congeners.[16] There are different fractionations and bioaccumulations between linear and branched PFOS in water, sediment, and biota collected from Lake Ontario.[15b] The perfluoroalkyl chains of these materials have unique properties. They possess weak intermolecular interactions due to the low polarizability of fluorine. Surface activity and the unique hydrophobic and lipophobic character of perfluorinated compounds results in the compounds having high thermal, chemical, and biological inertness because of the extreme stability of the carbon−fluorine bond.[44] However, the absence of pure authentic standards for the various congeners prevents more comprehensive NMR investigations into the congener-specific physical−chemical and toxicological properties of PFCAs. It is difficult to isolate and monitor them experimentally. Many of the current limitations in

---

[*] Corresponding author. Tel: (+1) 519-824-4120. Fax: (+1) 519 766 1499. E-mail: jgoddard@uoguelph.ca.

[†] University of Guelph.

[‡] Inner Mongolia Normal University.

10.1021/jp9078037 CCC: $40.75

TABLE 1: ^{19}F NMR Data for the Linear and Mono-trifluoromethyl Perfluoro-hexa-alkane Carboxylic Acids (Chemical Shifts in ppm)

No	isomer	atoms	predicted chemical shifts	predicted average chemical shift	chemical shift from experiment	helix twist angle
1	$CF_3^f\text{-}CF_2^e\text{-}CF_2^d\text{-}CF_2^c\text{-}CF_2^b\text{-}CF_2^a\text{-}COOH$	F^a	-118.75, -132.64	-125.70	-118.78	16.3$^{\blacktriangle}$
		F^b	-126.21, -130.86	-128.54	-121.50	
		F^c	-128.26, -127.82	-128.04	-122.55	
		F^d	-126.27, -129.50	-127.89	-122.55	
		F^e	-128.28, -136.70	-132.49	-125.98	
		F^f	-85.87, -90.21, -90.13	-88.74	-80.99	
2	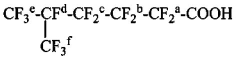 $CF_3^e\text{-}\underset{\overset{\vert}{CF_3^f}}{CF^d}\text{-}CF_2^c\text{-}CF_2^b\text{-}CF_2^a\text{-}COOH$	F^a	-117.39, -130.97	-124.18	-118.44	10.2$^{\blacktriangle}$
		F^b	-127.64, -126.36	-127.00	-121.76	14.1*
		F^c	-127.28, -119.43	-123.36	-114.36	6.3**
		F^d	-186.58	-186.58	-184.30	
		F^e	-76.16, -78.32, -80.78	-78.42	-71.84	
		F^f	-76.88, -77.76, -80.16	-78.27	-71.84	
3	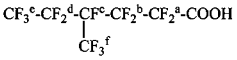 $CF_3^e\text{-}CF_2^d\text{-}\underset{\overset{\vert}{CF_3^f}}{CF^c}\text{-}CF_2^b\text{-}CF_2^a\text{-}COOH$	F^a	-121.14, -129.25	-125.20		23.1$^{\blacktriangle}$
		F^b	-121.15, -121.25	-121.20		4.7*
		F^c	-184.68	-184.68		41.6**
		F^d	-118.67, -121.37	-120.02		
		F^e	-84.65, -88.16, -89.50	-87.44		
		F^f	-75.33, -76.57, -78.32	-76.74		
4	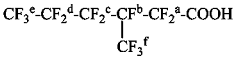 $CF_3^e\text{-}CF_2^d\text{-}CF_2^c\text{-}\underset{\overset{\vert}{CF_3^f}}{CF^b}\text{-}CF_2^a\text{-}COOH$	F^a	-115.36, -118.20	-116.78		10.5$^{\blacktriangle}$
		F^b	-184.40	-184.40		7.4*
		F^c	-123.12, -123.25	-129.19		13.5**
		F^d	-129.91, -135.89	-132.90		
		F^e	-66.86, -89.11, -89.88	-81.95		
		F^f	-76.39, -77.61, -77.69	-77.23		
5	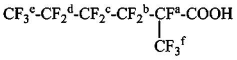 $CF_3^e\text{-}CF_2^d\text{-}CF_2^c\text{-}CF_2^b\text{-}\underset{\overset{\vert}{CF_3^f}}{CF^a}\text{-}COOH$	F^a	-184.87	-184.87		10.1$^{\blacktriangle}$
		F^b	-118.75, -125.23	-121.99		6.2*
		F^c	-126.06, -129.24	-127.65		14.0**
		F^d	-127.19, -134.72	-130.96		
		F^e	-85.66, -89.73, -90.20	-88.53		
		F^f	-76.72, -79.62, -80.70	-79.01		

Note: the shielding σ_{ref} of $CFCl_3$ calculated by the same methods is 179.19ppm.

All experimental data is from reference (42).

The $^{\blacktriangle}$ data are the average of the dihedral angles involved.

The " *" and "**" are the dihedral angles $D(C^d\text{-}C^c\text{-}C^b\text{-}C^a)$ and $D(C^e\text{-}C^d\text{-}C^c\text{-}C^b)$ in the chain

(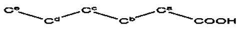). See the labels given above.

understanding the congener-specific environmental chemistry and toxicology of PFCAs are due to the absence of appropriate analytical methods.[15,24]

^{19}F NMR has been studied previously by the methods of quantum chemistry.[32,33] Quantum chemical investigations have become an important tool for the interpretation of experimentally obtained NMR spectra,[32,33] and examples of ^{19}F NMR chemical shift calculations can be found in the literature.[45−51] More recently, The^{19}F NMR of linear and branched perfluorooctanesulfonamides (PFOSAmide) have been predicted by density functional theory (DFT).[52] The predictions were consistent with experiment. To help detect and offer necessary information to the experimentalist about the ^{19}F NMR of *n*-alkane (C_6−C_8) PFCAs, and especially for the large numbers of branched isomers, we predict the ^{19}F NMR chemical shifts of 69 linear and branched PFCAs, $C_nF_{2n+1}COOH$ ($n = 6-8$) using DFT.

2. Computational Methods

Density functional theory predictions were made using the Gaussian 03 program package.[53] All geometries were optimized in the gas phase with the B3LYP hybrid functional and the 6-31G(d,p) basis set. Calculation of the Hessian indicates that all optimized geometries are local minima with no imaginary vibrational frequencies. ^{19}F shielding tensors for the 69 species were determined with the GIAO-B3LYP/6-31++G(d,p) method, which has proven accurate for the NMR properties of perfluorooctanesulfonamide.[52] The chemical shifts (δ) were derived from the shieldings (σ) by

$$\delta = \sigma_{\mathrm{ref}} - \sigma$$

where σ_{ref} is the F shielding in $CFCl_3$ predicted by the same methods. The contributions to the shieldings from the bond, core, and lone pair electrons were analyzed by the natural bond orbital method using the NBO3.1 program.[54]

3. Results

A total of 69 linear and branched C_6 to C_8 PFCAs, including 3 linear, 15 mono-trifluoromethyl branched, 31 ditrifluoromethyl branched, 13 tritrifluoromethyl branched, and 7 quad-trifluoromethyl branched with the empirical formula $C_nF_{2n+1}COOH$ were examined. The predicted data and available experimental results[42] for these compounds are summarized in Tables 1, 2, and 3 or in Supporting Information Tables S1, S2, and S3.

4. Discussion

4.1. Helical Structure of the Linear Isomers. After geometry optimizations, the linear *n*-alkane (C_6−C_{27}) PFCAs were predicted to have helical structures similar to perfluorinated *n*-alkanes,[23,55−58] (C_nF_{2n+2}), perfluorooctanesulfonate (PFOS),[52,59]

TABLE 2: ^{19}F NMR Data for the Linear and Mono-trifluoromethyl Perfluoro-hepta-alkane Carboxylic Acids (Chemical Shifts in ppm)

No.	isomers	atoms	predicted chemical shifts	predicted average chemical shift	chemical shift from experiment	helix twist angle
6	$CF_3^g\text{-}CF_2^f\text{-}CF_2^e\text{-}CF_2^d\text{-}CF_2^c\text{-}CF_2^b\text{-}CF_2^a\text{-}COOH$	F^a	-119.36, -131.88	-125.62	-118.76	$16.6^{\blacktriangle}$
		F^b	-126.68, -130.49	-128.59	-121.29	
		F^c	-128.01, -128.31	-128.16	-121.66	
		F^d	-127.03, -128.23	-127.63	-122.39	
		F^e	-126.07, -129.44	-127.76	-122.51	
		F^f	-128.10, -136.63	-132.37	-125.95	
		F^g	-85.80, -90.41, -90.69	-88.97	-80.94	
7	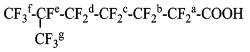 $CF_3^f\text{-}\underset{CF_3^g}{CF^e}\text{-}CF_2^d\text{-}CF_2^c\text{-}CF_2^b\text{-}CF_2^a\text{-}COOH$	F^a	-118.21, -133.30	-125.76	-118.69	$12.8^{\blacktriangle}$
		F^b	-123.56, -129.84	-126.70	-122.07	17.3*
		F^c	-125.32, -130.00	-127.66	-125.78	14.7^{**}
		F^d	-119.17, -127.32	-123.25	-114.57	6.3^{***}
		F^e	-185.54	-185.54	-185.73	
		F^f	-76.70, -77.93, -80.28	-78.30	-71.82	
		F^g	-76.09, -77.63, -80.82	-78.18	-71.82	
8	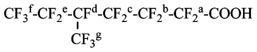 $CF_3^f\text{-}CF_2^e\text{-}\underset{CF_3^g}{CF^d}\text{-}CF_2^c\text{-}CF_2^b\text{-}CF_2^a\text{-}COOH$	F^a	-119.54, -132.90	-126.22		$20.4^{\blacktriangle}$
		F^b	-122.96, -127.02	-124.99		15.2^{*}
		F^c	-112.99, -119.19	-116.09		40.4^{**}
		F^d	-185.87	-185.87		5.7^{***}
		F^e	-125.53, -127.26	-126.40		
		F^f	-87.58, -88.52, -89.27	-88.46		
		F^g	-76.09, -76.91, -77.35	-76.78		
9	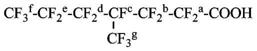 $CF_3^f\text{-}CF_2^e\text{-}CF_2^d\text{-}\underset{CF_3^g}{CF^c}\text{-}CF_2^b\text{-}CF_2^a\text{-}COOH$	F^a	-119.00, -128.75	-123.88		$20.5^{\blacktriangle}$
		F^b	-115.88, -115.90	-115.89		42.1^{*}
		F^c	-186.81	-186.81		5.1^{**}
		F^d	-122.71,- 123.64	-123.18		14.3^{***}
		F^e	-129.39, -133.57	-131.84		
		F^f	-84.87, -89.31, -90.60	-88.26		
		F^g	-76.38, -76.78, -77.01	-76.72		
10	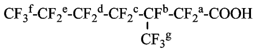 $CF_3^f\text{-}CF_2^e\text{-}CF_2^d\text{-}CF_2^c\text{-}\underset{CF_3^g}{CF^b}\text{-}CF_2^a\text{-}COOH$	F^a	-115.30, -117.36	-116.33		$12.8^{\blacktriangle}$
		F^b	-184.49	-184.49		7.0^{*}
		F^c	-120.70, -123.22	-121.96		14.9^{**}
		F^d	-129.20, -129.47	-129.34		16.6^{***}
		F^e	-125.64, -136.71	-131.18		
		F^f	-86.19, -90.27, -90.49	-88.98		
		F^g	-75.75, -76.90, -77.75	-76.80		
11	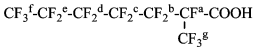 $CF_3^f\text{-}CF_2^e\text{-}CF_2^d\text{-}CF_2^c\text{-}CF_2^b\text{-}\underset{CF_3^g}{CF^a}\text{-}COOH$	F^a	-181.00	-181.00		$17.2^{\blacktriangle}$
		F^b	-114.84, -127.01	-120.93		17.9^{*}
		F^c	-125.13, -129.26	-127.20		18.0^{**}
		F^d	-125.40, -129.18	-127.29		16.6^{***}
		F^e	-128.25, -136.87	-132.56		
		F^f	-85.86, -90.31, -90.41	-88.86		
		F^g	-78.84, -79.05, -79.31	-79.07		

Note: the shielding σ_{ref} of $CFCl_3$ calculated by the same methods is 179.19ppm.

All experimental data is from reference (42).

The ▲ data are the average of the dihedral angles involved.

The " * ", " ** ", and " *** " are the dihedral angles D(C^d-C^c-C^b-C^a) , D(C^e-C^d-C^c-C^b), and D(C^f-C^e-C^d-C^c) in the carbon

chain (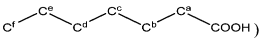) . See the labels given above.

perfluorooctanesulfonamide (PFOSAmide),[52] and perfluorocarboxylate anions.[60] Sketches of the optimized geometries of $C_6F_{13}COOH$, $C_7F_{15}COOH$, $C_8F_{17}COOH$, and $C_{27}F_{53}COOH$ are shown in Figure 1 and clearly reveal the helical structure.

As shown in Tables 1, 2, and 3 and in Figure 1, there are two carbon chains and four fluorine chains, all of which are helices in every optimized structure. The chains of carbons are termed the "odd chain" numbered from the first carbon next to COOH and "even chain" starting after that first carbon. The fluorine chain attached to odd numbered carbons next to COOH and nearest the CO group is "F chain 1", nearest the C−OH is "F chain 4". The fluorine chain on even numbered carbons and nearest the CO group is "F chain 2", nearest the C−OH is "chain 3". There are similar twist angles in the four helical optimized geometries for the linear isomers, with small differences depending on the chain length. The relation between the twist angle and the chain length is depicted in Figure 2.

As seen in Figure 2, the helical angle increases slightly with chain length, from 16.3° in $C_6F_{13}COOH$ to 17.2° in $C_{22}F_{45}COOH$. From $C_{22}F_{45}COOH$ at 17.2° to $C_{27}F_{55}COOH$ at 17.0°, there is only a very small change in this angle. These values are in good agreement with earlier calculated values of 15.3° for perfluorinated *n*-butane,[55] and 16.8° for $C_{10}F_{22}$.[58] The curve from $C_6F_{13}COOH$ to $C_{18}F_{37}COOH$ is steeper than from $C_{19}F_{37}COOH$ to $C_{27}F_{55}COOH$, where it flattens at an angle of approximately 17.0°. The results suggest that the helical twist angle has reached a limiting value when the carbon chain length is greater than about twenty seven. Nearly optimal values for a fluoropolymer are achieved at these chain lengths.

TABLE 3: ^{19}F NMR Data for the Linear and Mono-trifluoromethyl Perfluoro-octane-alkane Carboxylic Acids (Chemical Shifts in ppm)

No.	isomers	atoms	predicted chemical shift	predicted average chemical shift	chemical shift from experiment	helix twist angle
12	$\mathrm{CF_3^h\text{-}CF_2^g\text{-}CF_2^f\text{-}CF_2^e\text{-}CF_2^d\text{-}CF_2^c\text{-}CF_2^b\text{-}CF_2^a\text{-}COOH}$	F^a	-118.57, -131.69	-125.13	-117.56	16.6▲
		F^b	-126.11, -130.61	-128.36	-121.18	
		F^c	-127.64, -129.02	-128.33	-121.45	
		F^d	-128.29, -128.46	-128.38	-121.45	
		F^e	-124.80, -127.10	-125.95	-122.12	
		F^f	-126.53, -130.53	-128.53	-122.29	
		F^g	-128.60, -137.16	-132.88	-125.75	
		F^h	-85.27, -90.62, -90.72	-88.87	-80.64	
13	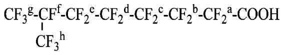 $\mathrm{CF_3^g\text{-}\underset{CF_3^h}{CF^f}\text{-}CF_2^e\text{-}CF_2^d\text{-}CF_2^c\text{-}CF_2^b\text{-}CF_2^a\text{-}COOH}$	F^a	-119.10, -134.83	-126.97	-117.48	13.9▲
		F^b	-125.34, -130.91	-128.13	-120.28	16.4*
		F^c	-125.81 -126.63	-126.22	-120.77	17.8**
		F^d	-125.71, -126.13	-125.92	-125.90	14.9***
		F^e	-113.11, -122.81	-117.76	-114.46	6.3****
		F^f	-189.35	-189.35	-185.50	
		F^g	-80.51, -80.51, -80.91	-80.64	-71.59	
		F^h	-78.18, -78.27, -79.08	-78.51	-71.59	
14	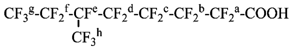 $\mathrm{CF_3^g\text{-}CF_2^f\text{-}\underset{CF_3^h}{CF^e}\text{-}CF_2^d\text{-}CF_2^c\text{-}CF_2^b\text{-}CF_2^a\text{-}COOH}$	F^a	-118.07, -133.78	-125.93		17.3▲
		F^b	-124.95, -130.25	-127.60		7.3*
		F^c	-124.14, -125.21	-124.68		15.7**
		F^d	-112.90, -119.00	-115.95		40.5***
		F^e	-186.22	-186.22		5.7****
		F^f	-125.52, -127.06	-126.29		
		F^g	-87.62, -88.55, -89.50	-88.56		
		F^h	-75.97, -76.53, -77.54	-76.68		
15	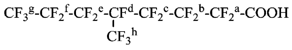 $\mathrm{CF_3^g\text{-}CF_2^f\text{-}CF_2^e\text{-}\underset{CF_3^h}{CF^d}\text{-}CF_2^c\text{-}CF_2^b\text{-}CF_2^a\text{-}COOH}$	F^a	-116.94, -134.07	-125.51		18.7▲
		F^b	-125.95, -127.89	-126.92		14.8*
		F^c	-120.71, -124.15	-122.43		5.0**
		F^d	-186.49	-186.49		41.6***
		F^e	-115.36, -117.84	-116.60		13.2****
		F^f	-128.00, -133.21	-130.61		
		F^g	-85.88, -89.25, -89.98	-88.37		
		F^h	-76.40, -76.54, -76.75	-76.56		
16	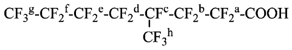 $\mathrm{CF_3^g\text{-}CF_2^f\text{-}CF_2^e\text{-}CF_2^d\text{-}\underset{CF_3^h}{CF^c}\text{-}CF_2^b\text{-}CF_2^a\text{-}COOH}$	F^a	-121.54, -131.32	-126.43		19.2▲
		F^b	-122.17, -124.38	-123.28		5.1*
		F^c	-186.08	-186.08		40.8**
		F^d	-113.60, -118.44	-116.02		15.1***
		F^e	-125.69, -126.32	-125.69		15.8****
		F^f	-129.06, -135.63	-132.35		
		F^g	-86.20, -90.10, -90.90	-89.07		
		F^h	-75.16, -75.75, -77.50	-76.14		
17	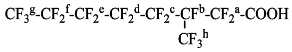 $\mathrm{CF_3^g\text{-}CF_2^f\text{-}CF_2^e\text{-}CF_2^d\text{-}CF_2^c\text{-}\underset{CF_3^h}{CF^b}\text{-}CF_2^a\text{-}COOH}$	F^a	-115.08, -117.76	-116.42		14.0▲
		F^b	-184.57	-184.57		7.0*
		F^c	-120.73, -123.79	-122.26		14.9**
		F^d	-126.69, -130.41	-128.55		18.1***
		F^e	-123.87, -130.14	-127.01		16.0****
		F^f	-128.19, -137.34	-132.77		
		F^g	-86.27, -90.50, -90.71	-89.16		
		F^h	-75.13, -77.07, -77.85	-76.68		
18	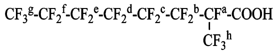 $\mathrm{CF_3^g\text{-}CF_2^f\text{-}CF_2^e\text{-}CF_2^d\text{-}CF_2^c\text{-}CF_2^b\text{-}\underset{CF_3^h}{CF^a}\text{-}COOH}$	F^a	-181.09	-181.09		17.8▲
		F^b	-115.93, -126.02	-120.98		17.5*
		F^c	-124.61, -128.74	-126.68		18.1**
		F^d	-124.85, -127.31	-126.08		17.6***
		F^e	-126.67, -130.07	-128.37		15.5****
		F^f	-128.61, -137.00	-132.81		
		F^g	-85.71, -90.33, -90.63	-88.89		
		F^h	-79.12, -79.15, -79.29	-79.19		

Note: the shielding σ_{ref} of $CFCl_3$ calculated by the same methods is 179.19ppm.

All experimental data is from reference (42).

The ▲ data are the average of the dihedral angles involved.

The " * ", " ** ", " *** ", and " **** " are the dihedral angles $D(C^d\text{-}C^c\text{-}C^b\text{-}C^a)$, $D(C^e\text{-}C^d\text{-}C^c\text{-}C^b)$, $D(C^f\text{-}C^e\text{-}C^d\text{-}C^c)$, and $D(C^g\text{-}C^f\text{-}C^e\text{-}C^d)$ in the carbon chain (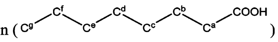) See the labels given above.

As shown in Tables 1, 2, and 3 or in Supporting Information Tables S1, S2, and S3, the branched isomer structures are similar overall to the linear ones. However, the dihedral angles in the branched structures differ due to a loss of approximate symmetry in the four carbon chain caused by the presence of a CF_3 substituent. For example, the unsymmetrical structures of $-CF_2-CF\ (CF_3)-CF_2-CF_2-$ in isomers 9, 14, 15, and 16 (see Tables 2 and 3) have larger dihedral angles, 42.1°, 40.5°, 41.6°, and 40.8°, respectively. Those of $-CF_2-CF_2-CF(CF_3)-CF_2-$ in isomers 31, 49, and 51 (see Supporting Information Tables S2 and S3), have dihedral angles of 43.4°, 48.0°, and 42.7°, respectively.

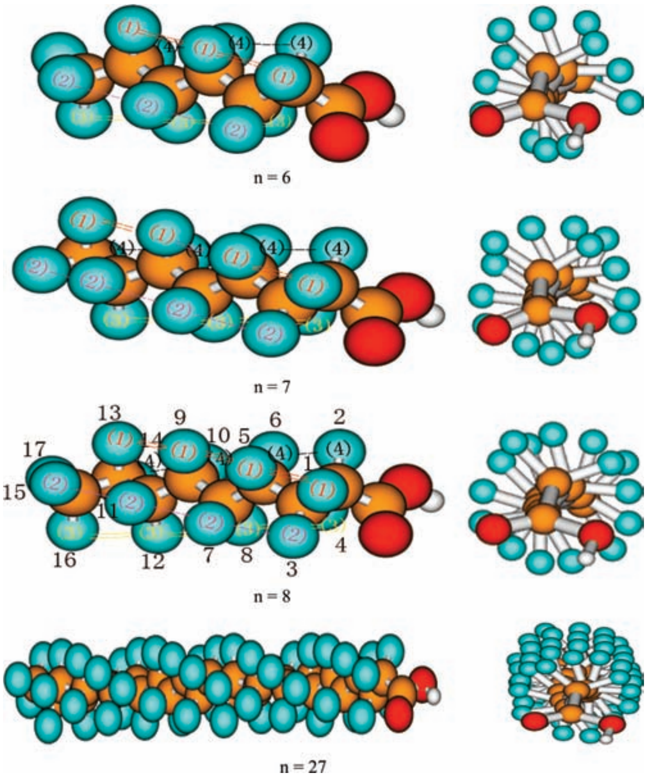

Figure 1. Helical optimized geometries of $C_6F_{13}COOH$, $C_7F_{15}COOH$, $C_8F_{17}COOH$, and $C_{27}F_{55}COOH$ (for $n = 6$, 7, and 8). The four fluorine chains are labeled 1, 2, 3, and 4.

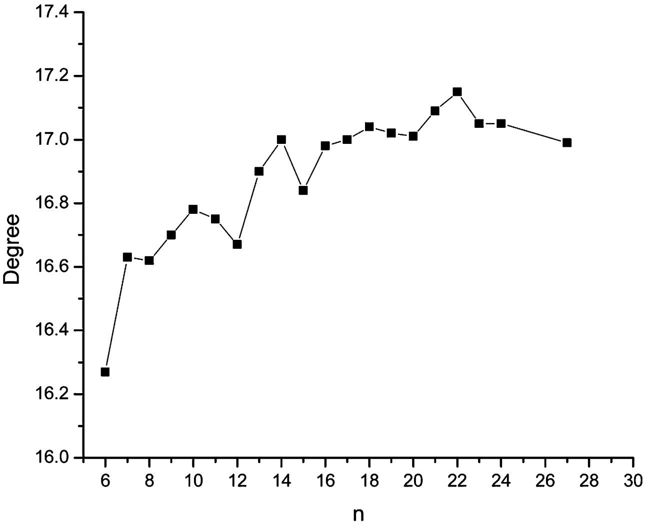

Figure 2. Average helical angle as a function of carbon chain length in the linear C_6-C_{27} perfluorinated alkanecarboxylic acids.

4.2. Trends in ^{19}F Chemical Shifts. Examination of the tables and of other reports[14,35] reveal that the chemical shifts of perfluoro compounds can be organized on the basis of functional group. All resonances of a particular group (e.g., CF_3, CF_2, CF) cluster together and are further subdivided by empirical formula or by neighboring functional groups (e.g., isopropyl branched, internally mono-trifluoromethyl branched, tertiary butyl, α-trifluoromethyl branched, internally ditrifluoromethyl branched, internally neighboring-ditrifluoromethyl branched, α-trifluorodimethyl branched, etc.).

4.2.1. Trifluoromethyl Group (CF_3). In the linear isomers (1, 6, 12) in Tables 1, 2, and 3, three ^{19}F chemical shifts were predicted for the terminal CF_3. The average values for the these shifts in the three isomers are −85.65, −90.41, and −90.51 ppm. The average of the three average values is −88.86 ppm, as compared to the experimental value of −80.86 ppm.[42] The plot of the ^{19}F chemical shifts in the terminal CF_3 vs increasing chain length is shown in Supporting Information S-Figure 1 for the linear isomers. There are very small changes in the predicted or experimental ^{19}F chemical shifts with increasing chain length.

For the branched isomers in the tables, overall, the ^{19}F chemical shifts for the fluorines in the branched CF_3 are smaller in magnitude than the terminal CF_3 in the linear isomers. The decrease is correlated with the steric hindrance of the CF_3 group. The more hindered the CF_3 group, the smaller are the ^{19}F chemical shifts. For example, for the isomers 44, 67, and 68 (see Supporting InformationTables S2 and S3), with sterically hindered CF_3 groups, the ^{19}F chemical shifts in the CF_3 groups are range from −60 to −70 ppm, lower by about 20 ppm than those of the terminal CF_3 in linear isomers. For 15 mono-trifluoromethyl branched isomers, plots of the average ^{19}F NMR chemical shifts in the terminal and branched CF_3 of the mono-methyl branched isomers vs the branching site are shown in Supporting Information S-Figures 2 and 3, respectively.

As shown in Supporting Information S-Figures 2 and 3, the trends in the average ^{19}F NMR chemical shifts in the terminal or branched CF_3 are consistent in the mono-trifluoromethyl branched perfluorohexanecarboxylic acids, mono-trifluoromethyl branching perfluoroheptanecarboxylic acids, and mono-trifluoromethyl branched perfluorooctanecarboxylic acids. For the terminal CF_3, except for the isopropyl branched isomers (2, 7, 13), the average ^{19}F NMR shifts show no change with the site of the internal branching. The value is approximately −88.59 ppm. However, in the three isopropyl branched isomers (2, 7, 13), the average ^{19}F NMR shifts (−78.41 ppm in the terminal CF_3 groups) are 10 ppm smaller in magnitude compared to the shifts of other mono-trifluoromethyl internal branched isomers.

For the branching CF_3 in the branched isomers, the average ^{19}F chemical shifts show no change with the site of the internal branching except for the isopropyl branched isomers (2, 7, 13) and α-trifluoromethyl branched isomers (5, 11, 18). The value is approximately −76.70 ppm, obviously smaller in magnitude than the corresponding value in the terminal CF_3 by approximately 12 ppm. However, in the three isopropyl branched isomers (2, 7, 13), the values (−78.32 ppm) are larger by about 2 ppm compared to the corresponding values in the other mono-trifluoromethyl internal branched isomers. In the three α-trifluoromethyl branched isomers (5, 11, 18), the values (−79.09 ppm) in the branching CF_3 are larger by about 2 ppm compared to the values for other mono-trifluoromethyl internal branched isomers.

4.2.2. Difluoromethylene Group (CF_2). For the linear isomers (1, 6, 12), the ^{19}F chemical shifts in the CF_2 groups are presented in Tables 1, 2, and 3. In $C_6F_{13}COOH$, $C_7F_{15}COOH$, and $C_8F_{17}COOH$, the average ^{19}F chemical shifts for all the CF_2 groups are close at −128.16, −128.04, and −127.91 ppm, respectively. These values are within 6.21 ppm of experiment.[42] The values decrease with increasing chain length with the exception of the α-CF_2 and the CF_2 next to the terminal CF_3. For the α-CF_2, the corresponding values are −125.70, −125.62, and −125.13 ppm, respectively, and are within 7.57 ppm of experiment.[42] The small differences may be attributed to the effects of solvent. Isolated PFCAs are calculated, but experiments are in solution.[42] Opposite to the case of the α-CF_2, the values for the CF_2 next to the terminal CF_3 are larger than for the other CF_2 groups, at −132.49, −132.47, and −132.58 ppm,

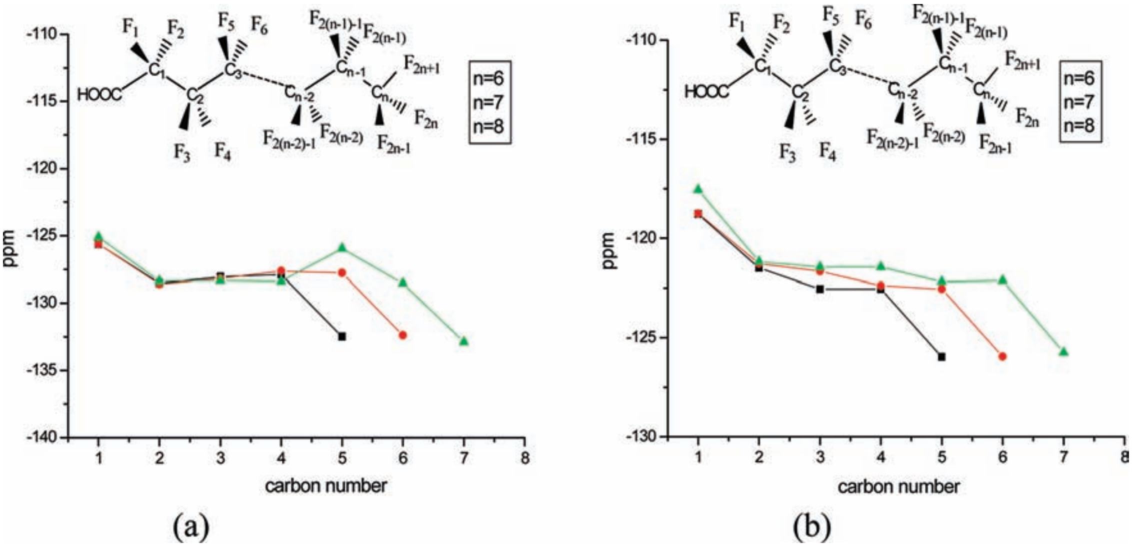

Figure 3. Average ^{19}F chemical shifts in the CF_2 groups with the increasing number of carbons: (a) prediction: (b) experiment.

TABLE 4: Contributions to the ^{19}F Isotropic Shieldings from F Core (CR), F Lone Pair (F LP), C−F Bonding Electrons (C−F BD), Other Bonding Electrons, and Other Lone Pairs

		contributions (ppm)					
			$\sum_i$ (BD)		$\sum$ (LP)		
CF_2 Sites	atoms	CR	C−F BD	other BD	F LP	other LP	total (ppm)
α	F_1	311.94	79.06	−28.47	−51.11	−14.19	297.23
	F_2	331.94	−7.35	−7.33	24.93	−12.37	309.82
Central	F_7	311.96	60.62	−6.36	−32.16	−24.51	309.55
	F_8	311.96	63.67	−7.03	−33.79	−25.88	308.93
Next to CF_3	F_{13}	311.94	−5.85	−7.67	26.26	−6.46	318.22
	F_{14}	311.95	60.45	−19.57	−21.87	−21.87	309.09

respectively. The small differences of chemical shifts in the geminal fluorines for the CF_2 next to the terminal CF_3 may be the result of the difference between chiral carbons.

The trends in predicted and experimental average ^{19}F chemical Shifts in CF_2 with the increasing number of carbons are shown in Figure 3a,b, respectively. As shown in these figures, the values of the CF_2 chemical shifts are near the experimental ones although larger than experiment. The trends in both quantities with the number of carbons are very similar.

Two different ^{19}F chemical shifts in the CF_2 groups were predicted. There are different interactions between the two fluorine atoms bonded to the same carbon in the helical conformation. The ^{19}F chemical shifts for CF_2 for the odd- and even-carbon chains of the linear perfluoro-carboxylic acids $C_6F_{13}COOH$, $C_7F_{15}COOH$, and $C_8F_{17}COOH$, are depicted in Supporting Information S-Figure 4a−c, respectively. In these conformations, there are similar trends. In the center of both the odd- and even-carbon helical chains, the ^{19}F chemical shifts are very similar. At the ends of the chains, there are larger differences in the ^{19}F chemical shifts. For example, for the α-CF_2 in $C_6F_{13}COOH$, $C_7F_{15}COOH$, and $C_8F_{17}COOH$, the average values for the fluorines on the odd-carbon chain (see Figure 1) are −118.75, −119.36, and −118.75 ppm, respectively, whereas the average values in the even-carbon chain are −132.64, −131.88, and −131.69 ppm. In the CF_2 next to the terminal CF_3 in $C_6F_{13}COOH$, $C_7F_{15}COOH$, and $C_8F_{17}COOH$, the values for the fluorines on the odd-carbon chain are −128.28, −128.10, and −128.60 ppm, whereas the average values for fluorines on the even-carbon chain are −136.70, −136.63, and −137.16 ppm.

To reveal the causes of these differences, the contributions to the shielding for the bonding, core, and lone pair (p) electrons were predicted with the NBO 3.1 program. On the basis of the contributions to the ^{19}F isotropic shielding using natural localized molecular orbital (NLMO),[54,61] the ^{19}F isotropic shieldings are divided into F core (CR), lone pair (LP), and bond (BD) terms.

$$\sigma_{\mathrm{sum}} = \sigma(\mathrm{CR}) + \sum \sigma_i(\mathrm{BD}) + \sum \sigma_j(\mathrm{LP})$$

j is the sum over all lone pair electrons, and i is the sum over all covalent bonds. The results for these contributions to the ^{19}F isotropic shielding of the central CF_2, α-CF_2, and the CF_2 next to the terminal CF_3 in the odd- and even-carbon chains for $C_8F_{17}COOH$ are listed in Table 4 and shown in Figures 4 and 5, and Supporting Information S-Figures 5−8. The F_7 and F_8 atoms are on the central CF_2 in the odd- and even-carbon chains, respectively. F_1 and F_2 are in the α-CF_2 for the odd and even chains. F_{13} and F_{14} are on the CF_2 next to the terminal CF_3 for the odd and even chains.

As seen in Table 4, Figures 4a and 5a, and Supporting Information S-Figure 5a−8a, the ^{19}F shielding σ_{sum} is dominated by the contribution of the F core orbitals. The contributions of the F core to the different F atoms are almost equations, and approximately 311.95 ppm. The different ^{19}F chemical shieldings are caused by the different contributions of the bonds and lone pairs. The ^{19}F shieldings of F_7 and F_8 on the central CF_2 (see Figures 4 and 5), are very similar. The contributions of the F core (CR), F lone pair electrons (F LP), C−F bonding electrons (C−F BD), other bonding electrons, and other lone pair electrons (ppm) to the shieldings of F_7 and F_8 are all very similar, the differences of the quantities between F_7 and F_8 are 0.00, +1.63,

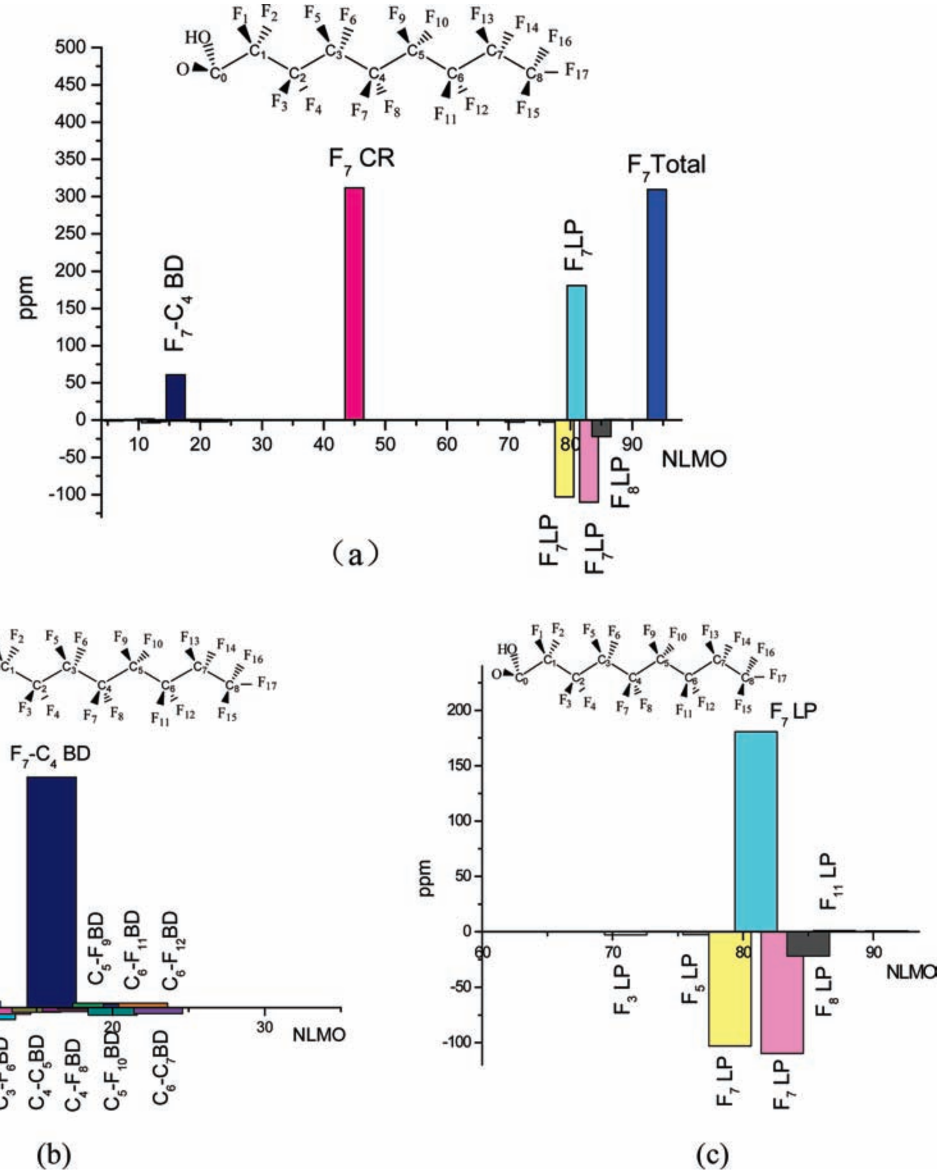

Figure 4. Contributions to shieldings for F_7 on the central CF_2 with natural local molecular orbital (NLMO) in $C_8F_{17}COOH$: (a) total distribution; (b) bond distribution; (c) lone pair distribution.

−3.05, +0.67, and +1.37 ppm, respectively. The chemical shifts of F_7 and F_8, are nearly identical.

For the ^{19}F shieldings of F_1 and F_2 in the α-CF_2, see Table 4 and S-Figures 5 and 6. They are in different surroundings, with F_1 closer to the oxygen in the carbonyl (CO) ($r(F_1-O) = 2.744$ Å, $r(F_1-OH) = 3.422$ Å), whereas F_2 is closer to the hydroxyl oxygen ($r(F_2-O) = 3.496$ Å, $r(F_1-OH) = 2.564$ Å). Thus there are different interactions. The contributions of the F core (CR), F lone pair electrons (F LP), C−F bonding electrons (C−F BD), other bonding electrons, and other lone pair electrons (ppm) for F_1 and F_2 all are different. The different ^{19}F shieldings are determined by the contributions of the bonds and lone pairs.

Comparing Supporting Information S-Figure 5b,c with S-Figure 6b,c, there are markedly different contributions of the bond or lone pairs to the chemical shifts for F_1 and F_2. First, the contributions of the bonds are very different between the F_1-C_1 and F_2-C_1, +79.06 and −7.35 ppm, respectively. The sum of the contributions of the other bonds for F_1 is −28.47 ppm, but −7.33 ppm for F_2. The difference in all bond contributions is 65.27 ppm. This difference is between the sum of the F_1-C_1 and other bond contributions to F_1 and the sum of the F_2-C_1 and other bonds for F_2. For the lone pair contributions, there are also obvious differences between F_1 and F_2. The sum of the differences of all the lone pair contributions is 77.86 ppm involving the sum of the F_1 three lone pairs and other lone pair contributions for F_1 and the sum of the F_2 three lone pairs and other lone pairs to F_2. The three lone pairs contribute −51.11 and +24.93 ppm to F_1 and F_2, respectively. The sum of the other lone pair contributions for F_1 is −14.19 ppm, while it is −12.37 ppm for F_2. Especially, there are different lone pair contributions from the neighboring fluorine. The contribution to F_1 from its neighbor F_2 is −11.90 ppm, but for F_2 from its neighbor F_1 is −2.50 ppm. Furthermore, there are different lone pair contributions from the neighboring oxygen. The contribution at F_1 from the oxygen in the carbonyl is −0.92 ppm. For F_2 from the oxygen in the carbonyl and in the hydroxyl the contributions are −6.33 and −4.28 ppm, respectively.

For the ^{19}F chemical shieldings of F_{13} and F_{14} in the terminal CF_2 (see Table 4 and Supporting Information S-Figures 7 and 8), there are different interactions. F_{14} is closer to the terminal CF_3 and the C_7-C_8 bond than F_{13}, ($r(F_{14}-F_{15}) = 3.508$ Å,

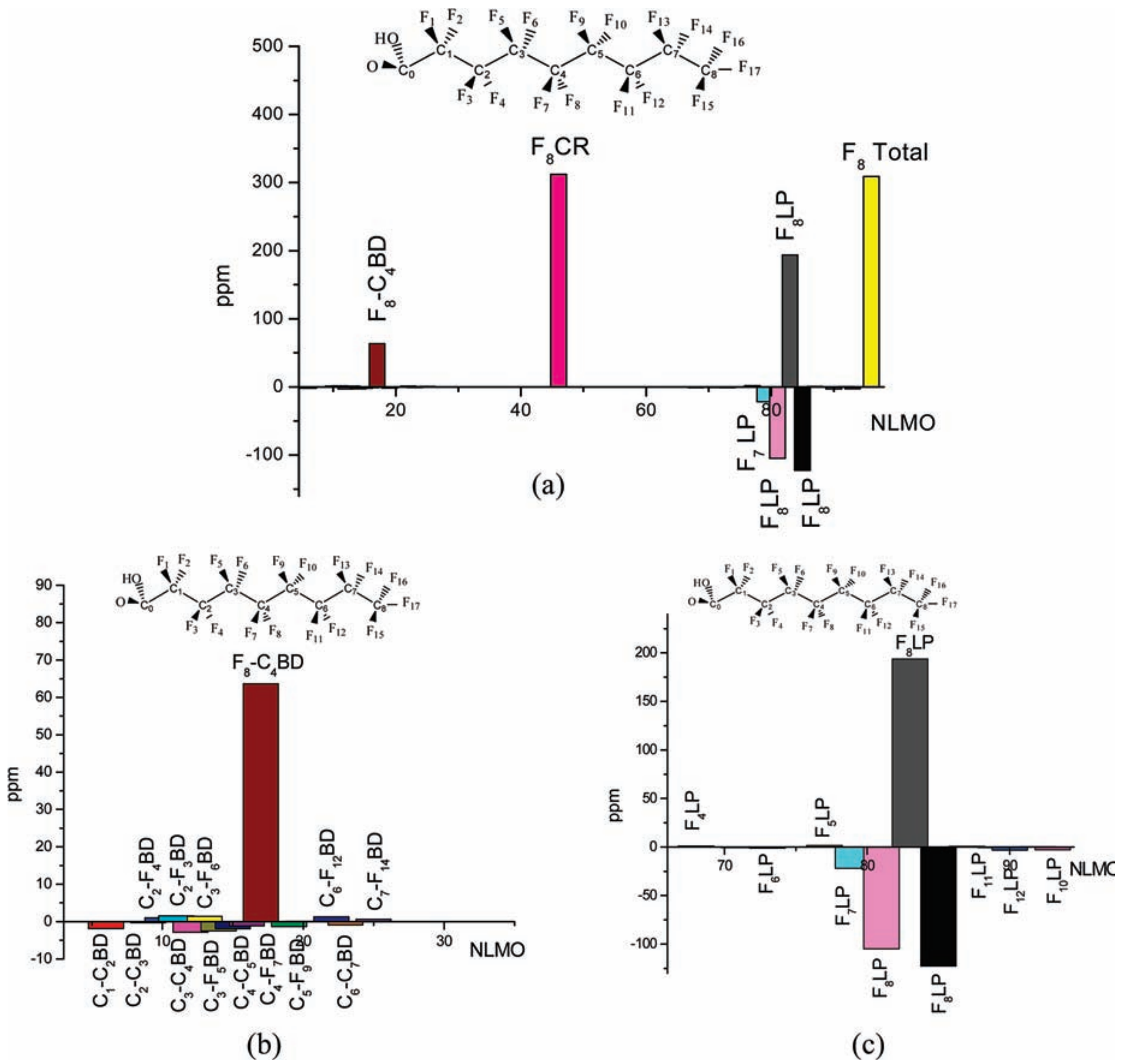

Figure 5. Contributions to shieldings for F_8 on the central CF_2 with natural local molecular orbital (NLMO) in $C_8F_{17}COOH$: (a) total distribution; (b) bond distribution; (c) lone pair distribution.

$r(F_{14}-F_{16}) = 2.842$ Å, $r(F_{14}-F_{17}) = 2.620$ Å, $r(F_{14}-C_7) = 1.351$ Å, and $r(F_{14}-C_8) = 2.349$ Å, while $r(F_{13}-F_{15}) = 2.666$ Å, $r(F_{13}-F_{16}) = 3.515$ Å, $r(F_{13}-F_{17}) = 2.802$ Å, $r(F_{13}-C_7) = 1.354$ Å, and $r(F_{13}-C_8) = 2.349$ Å There is a 9.13 ppm difference in the total ^{19}F chemical shieldings. The contributions of the F core (CR), F lone pair electrons (F LP), C−F bonding electrons (C−F BD), other bonding electrons, and other lone pair electrons to F_{13} and F_{14} are very different. Comparing Supporting Information S-Figure 7b,c with S-Figure 8b,c, there are markedly different contributions of the bond and lone pairs to the shieldings for F_{13} and F_{14}. First, the contributions of the bonds are very different between the $F_{13}-C_7$ and $F_{14}-C_7$, −5.85 and +60.45 ppm, respectively. The sum of the other bond contributions to F_{13} is −7.67 ppm, but −19.57 ppm for F_{14}. The C_7-C_8 bond contribution to F_{13} is −11.94 ppm, but for F_{14} it is −16.71 ppm. The sum of the difference of all bond contributions is 54.40 ppm between the sum of the $F_{13}-C_7$ and other bond contributions to F_{13} and the sum of the $F_{14}-C_7$ and other bond contributions to F_{14}. The lone pair contributions to F_1 and F_2 are obviously different. The sum of the difference of all the lone pair contributions is 63.54 ppm. This difference is between the sum of the F_{13} three lone pairs and other lone pair contributions to F_{13} and the sum of the F_{14} three lone pairs and other lone pair to F_{14}. The three lone pairs contribute +26.26 and −21.87 ppm to F_{13} and F_{14}, respectively. The sum of the other lone pair contributions is −7.67 ppm, and −19.57 ppm to F_{13} and F_{14}. The contribution for F_{13} from its neighbor F_{14} is −3.88 ppm, but for F_{14} from F_{13} it is −13.59 ppm. Furthermore, there are different lone pair contributions from the CF_3 between F_{13} and F_{14}. The contribution for F_{13} from the CF_3 is −3.73 ppm, but for F_{14} is −7.46 ppm. There are obviously different ^{19}F shieldings between the F_{13} and F_{14}.

The trends of the ^{19}F chemical shifts in the four different fluorine helical chains are depicted in Supporting Information S-Figures 9 and 10. As shown in Supporting Information S-Figure 9, the trends in the ^{19}F chemical shifts for the CF_2 in the four fluorine helical chains are not identical. The absolute values in the 1 and 3 F chains increase with increasing distance between the fluorine atom and the carboxylic acid group (see Supporting Information S-Figure 9a,c). The absolute values in the 2 and 4 chains first decrease, then slightly increase. These changes are related to the distance between the initial fluorine atom in the F helical chain and the oxygen atoms in the carbonyl or hydroxyl groups. For example, in linear $C_8F_{17}COOH$, the distance between the first fluorine atom (F_1) in F chain 1 and the oxygen atoms in the carbonyl and hydroxyl groups are

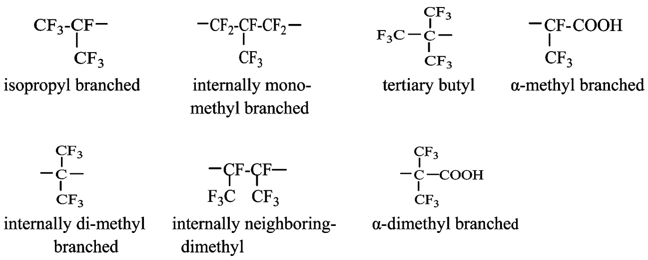

Figure 6. Seven characteristic groups.

$r(F_1{-}O_{C=O}) = 2.744$ Å and $r(F_1{-}O_{O-H}) = 3.422$ Å, respectively. The corresponding distance in chain 3 is $r(F_4{-}O_{C=O}) = 3.413$ Å, $r(F_4{-}O_{O-H}) = 3.062$ Å, in the chain 2 $r(F_3{-}O_{C=O}) = 3.098$ Å, $r(F_3{-}O_{O-H}) = 4.067$ Å, and in chain 4 $r(F_2{-}O_{C=O}) = 3.450$ Å, $r(F_2{-}O_{O-H}) = 2.564$ Å. Comparing the distance between the initial fluorine atom in the F chain and the oxygen atom in the carbonyl group, we find that the distances for chains 1 and 3 are shorter than for chains 2 and 4. The distance between the initial fluorine atom in the F chain and the oxygen atoms in the hydroxyl group for chains 2 and 4 are shorter than for chains 1 and 3. The ^{19}F chemical shifts for CF_2 in chains 1 and 3 are related to the interactions between the initial fluorine atom in the F chain and the oxygen atoms in the carbonyl group. The ^{19}F chemical shifts for CF_2 in chains 2 and 4 are related to interactions between the initial fluorine atom and the oxygen atoms in the hydroxyl group.

The trends in the ^{19}F chemical shifts for the CF_2 in the four fluorine chains for linear $C_6F_{13}COOH$, $C_7F_{15}COOH$, and $C_8F_{17}COOH$ are shown in Supporting Information S-Figure 10. The trends in the ^{19}F chemical shifts in the three linear perfluoro-carboxylic acids are similar, and the same as in Supporting Information S-Figure 4. There are large differences of the ^{19}F chemical shifts in the beginnings of the F chains 1 and 4 for the three linear perfluoro-carboxylic acids. The differences for the three compounds are 13.8, 12.5, and 13.1 ppm, respectively. There are large differences in the ^{19}F chemical shifts in the ends of the F helical chain between chains 1 and 4 for the linear perfluoro-carboxylic acids, including the even carbon atoms, or between the chains 2 and 3 for linear perfluoro-carboxylic acids including the odd carbon atoms. The differences for the three compounds are 8.4, 8.5, and 8.6 ppm, respectively. The effect of the carbonyl is greater than the trifluoromethyl group making the differences larger at the carboxylic acid end of the chain.

In the branched isomers (see Tables 1, 2, and 3 or Supporting Information Tables S1, S2, and S3), the ^{19}F chemical shifts in CF_2 are smaller than in the linear isomers, and the decrease is correlated with the extent of steric hindrance of the CF_3 group. The more hindered the CF_3 group, the smaller the ^{19}F chemical shifts in the CF_2. For example, the ^{19}F chemical shifts in the CF_2^b group in isomer 68 (see Supporting Information Table S3), having sterically hindered CF_3 groups, is only −87.15 ppm, lower by about 25 ppm than that of the CF_2 in the linear isomers.

4.2.3. Mono-fluoromethyl Group (CF). In the isopropyl branched isomers (2, 7, 13), the absolute average ^{19}F chemical shifts of the CF next to the terminal trifluoromethyl group (CF_3) is predicted to be 187 ppm, 2 ppm larger than experiment. The trends in the predicted ^{19}F chemical shifts of CF and in experiment are shown in Supporting Information S-Figure 11.

To reveal trends in the ^{19}F chemical shifts in CF, the ^{19}F chemical shifts of CF with the site of substitution of the trifluoromethyl group (CF_3) in 15 monosubstituted trifluoromethyl group (CF_3) isomers (2−5, 7−11, 13−18) are depicted in Supporting Information S-Figure 12.

As shown in Supporting Information S-Figure 12, the trends for $n = 6$, 7, and 8 are very similar. The value of the chemical shift of α-CF is smallest in magnitude, and there is a local maxmum at the center of the chain. The value of the shielding of the CF is larger compared to the F shielding in the CF_3. Although the ^{19}F chemical shifts in CF change with the site of substitution of the trifluoromethyl group (CF_3), the change is relatively small, from −181.0 to −189.4 ppm.

In the other branched isomers (see Supporting Information Tables S1, S2, and S3), the ^{19}F chemical shifts of CF are smaller in magnitude for the multibranched isomers than for the monobranched isomers. The decrease correlates with the steric hindrance of the CF_3 group. The more hindered the CF_3 group, the smaller the ^{19}F chemical shifts in the CF. For example, the ^{19}F chemical shifts of the CF^b group in isomer 64 (see Supporting Information Tables S3), with sterically hindered CF_3 groups, is only −158.17 ppm, lower by about 25 ppm than that of the CF in the mono- trifluoromethyl branched isomers.

4.2.4. Other Groups. Three perfluorooctanesulfonyl fluorides and perfluorooctanesulfonic acid produced industrially contain 73% of the linear, 10% of the isopropyl branched, 18% of the internally branched, and 0.3% of the tertiary butyl isomers.[14] The results of the NMR predictions for 69 isomers of three perfluoro-carboxylic acids are reported in this work (see Tables

TABLE 5: Average Values and Confidence Intervals of ^{19}F NMR in CF_3, CF_2, and CF Groups in Eight Blocks (Numbers of Structures in Brackets Summations over Numbers of Isomers)

blocks	groups	average (ppm)	standard deviation (S)	confidence interval[a]	experiment (ppm)
linear (3)	CF_3	−88.86	0.12	−88.47 to −89.25	−80.9[b]
	CF_2	−128.35	2.25	−126.83 to −129.87	−121.9[b]
isopropyl branched (21)	CF_3	−76.10	3.17	−74.14 to −78.06	−71.8[b]
	CF	−178.50	8.64	−173.16 to −183.84	−185.2[b]
internally mono-methyl branched (17)	CF_3	−76.55	0.51	−76.15 to −76.87	−70 to −72[c]
	CF_2	−118.68	4.74	−116.46 to −120.90	
	CF	−183.98	2.17	−182.46 to −185.50	−176 to −187[c]
tertiary butyl (9)	CF_3	−66.93	3.09	−63.58 to −70.28	−63[d], −66.5[d]
α-methyl branched (21)	CF_3	−77.60	3.51	−75.43 to −79.77	−75.2[d]
	CF	−176.93	7.03	−172.59 to −181.27	−172.2[d]
internally dimethyl branched (8)	CF_3	−66.13	1.48	−64.37 to −67.89	−64.1[d]
internally neighboring-dimethyl branched (17)	CF_3	−74.18	2.71	−72.28 to −76.08	−74.1, −75.0[d]
	CF	−175.09	6.75	−170.35 to −179.83	−179.8, −184.9[d]
α-dimethyl branched (9)	CF_3	−66.72	2.11	−64.43 to −69.01	

[a] Average $\bar{X} \mp (St)/(n^{1/2})$, where n is the sum of isomers, S is standard deviation, and t is critical value at 0.01 level in t test. [b] Average experimental data for the n-alkane (C_6−C_8) carboxylic acids.[42] [c] Experimental data for perfluorooctanesulfonic acid (PFOS).[14] [d] Experimental data for perfluorooctanesulfonamide (PFOSAmide).[39]

1, 2, and 3 or Supporting Information Tables S1, S2, and S3). Seven characteristic blocks are sketched in Figure 6, and the results of a statistical analysis of the normalized ^{19}F chemical shifts are presented in Table 5.

As seen from Table 5, there are very different ^{19}F chemical shifts in the same group, such as CF_3, CF_2, or CF, for the seven blocks. In general, the average magnitudes are smaller in the seven blocks than in the linear isomers. Especially, for the value of the CF_3 group, the change is more marked compared to the value for the terminal CF_3 in the linear isomers. For example, the ^{19}F chemical shift is approximately -66 ppm in nine tertiary butyl, eight internally dimethyl branched, and nine α-dimethyl branched isomers. This value is 22 ppm smaller than for the terminal CF_3 of the linear isomers. For the CF_2 and CF, the changes are not large and less than 10 ppm. Overall, the decease in chemical shift is related to the steric hindrance of the CF_3 groups. The more hindered is the CF_3 group, the larger is the decease of the ^{19}F chemical shift. In addition, comparing the predictions with experimental data shows a deviation of 8 ppm. The computational methods are reliable. Comparing the predictions with experiment for perfluorooctanesulfonic acid (PFOS),[14] and perfluorooctanesulfonamide (PFOSAmide),[39] with the different functional groups, $-COOH$, $-SO_3H$, $-SO_3NH_2CH_2CH_3$, the predicted ^{19}F chemical shifts are very similar. The effect of the different functional groups on the ^{19}F chemical shifts for the same structural blocks is very small for the same perfluorocarbon chain.

5. Conclusions

Full geometry optimizations for the linear *n*-alkane (C_6-C_{27}) PFCAs indicate helical structures. The helical angle increases slightly with increasing chain length, from 16.3° in perfluoro-hexa-alkane carboxylic acids ($C_6F_{13}COOH$) to 17.0° in $C_{27}F_{55}COOH$. The helical twist angle has nearly reached a limiting value when the carbon chain length is greater than about twenty seven.

The predictions of the ^{19}F chemical shifts for 69 linear and branched isomers of the perfluoro-carboxylic acids $C_6F_{13}COOH$, $C_7F_{15}COOH$, and $C_8F_{17}COOH$ are presented. There are differences in the ^{19}F chemical shifts among the CF_3, CF_2, and CF groups. In general, the values for the CF_3 group are smaller in magnitude than 90 ppm, the values for the CF group are larger in magnitude than 160 ppm, and the values in magnitude for the CF_2 group are between 110 ppm and 130 ppm. Comparing the values for the linear and the branched isomers shows the values in the latter are smaller. The decrease is correlated with the extent of steric hindrance of the CF_3 group. The more hindered the CF_3 group, the greater the decrease in the ^{19}F chemical shifts.

Statistically the ^{19}F chemical shifts, for isopropyl branched, internally mono-methyl branched, tertiary butyl α-methyl branched, internally dimethyl branched, internally neighboring-dimethyl, and α-dimethyl branched blocks, are smaller in magnitude than in the linear isomers. Comparing the predictions for PFCAs with analogous perfluoro compounds shows the predicted ^{19}F chemical shifts are similar. The effects of the different functional (e.g., $-COOH$, $-SO_3H$, $-SO_3NH_2CH_2CH_3$) groups on the ^{19}F chemical shift in the same structural blocks are very small for the same perfluorocarbon chains. Therefore, it is possible to use computer modeling to obtain chemical shift predictions in fluorine NMR which could extend to identification of novel fluorinated organics in the environment.

Many issues related to this study deserve further exploration, including solvent effects, NMR splitting patterns, and detailed comparisons of other predicted physical and chemical properties of linear and branched isomers, will lead to great understanding.

Acknowledgment. This research was supported by the Natural Sciences and Engineering Research Council of Canada (NSERC). Computational resources were provided by the Shared Hierarchical Academic Research Computing Network (SHARCNET).

Supporting Information Available: Tables and figures showing predicted ^{19}F NMR data for perfluoro-hexa-alkane, perfluoro-hepta-alkane, and perfluor-oocta-alkane carboxylic acids with multiple trifluoromethyl groups. This material is available free of charge via the Internet at http://pubs.acs.org.

References and Notes

(1) Simons, J. H. *J. Electrochem. Soc.* **1949**, *95* (2), 47–67.

(2) Kestner, T. A. *J. Fluorine Chem.* **1987**, *36*, 77–82.

(3) Huang, B. N.; Haas, A.; Lieb, M. *J. Fluorine Chem.* **1987**, *36*, 49–62.

(4) Sartori, P.; Ignat'ev, N. *J. Fluorine Chem.* **1998**, *87*, 157–162.

(5) Ignat'ev, N. V.; Welz-Biermanna, U.; Heider, U.; Kucheryna, A.; Ahsen, S. v.; Habel, W.; Sartori, P.; Willner, H. *J. Fluorine Chem* **2003**, *124*, 21–37.

(6) Velayutham, D.; Jayaraman, K.; Kulangiappar, K.; Ilayaraja, N.; Ram Babu, Y.; Santhan Rao, P.; Narayana Reddy, S.; Victor, Babu; Noel, K. M. *J. Fluorine Chem.* **2006**, *127*, 1111–1118.

(7) Lehmler, H. J. *Chemosphere* **2005**, *58*, 1471–1496.

(8) Kanno, N.; Tonokura, K.; Hurley, M. D.; Wallington, T. J. *J. Fluorine Chem.* **2008**, *129*, 1187–1192.

(9) Henne, A. L.; Alderson, T.; Newman, M. S. *J. Am. Chem. Soc.* **1945**, *67*, 918–919.

(10) Haszeldine, H. N. *Nature* **1950**, *166*, 192–193.

(11) Kauck, E. A.; Diesslin, A. R. *Ind. Eng. Chem.* **1951**, *43*, 2332–2334.

(12) Hauptschein, M.; Braid, M. *J. Am. Chem. Soc.* **1961**, *83*, 2500–2505.

(13) Hauptschein, M.; Braid, M. *J. Am. Chem. Soc.* **1961**, *83*, 2505–2507.

(14) Vyas, S. M.; Kania-Korwel, I.; Lehmler, H. J. *J. Envion. Sci. Health A* **2007**, *42*, 249–255.

(15) (a) Rayne, S.; Forest, K.; Friesen, K. J. *J. Envion. Sci. Health A* **2008**, *43*, 1391–1401. (b) Houde, M.; Czub, G.; Small, J. M.; Backus, S.; Wang, X.; Alaee, M.; Muir, D. C. G. *Environ. Sci. Technol.* **2008**, *42*, 9397–9403.

(16) Rayne, S.; Forest, K.; Friesen, K. J. *J. Mol. Struct.: THEOCHEM* **2008**, *869*, 81–82.

(17) Prevedouros, K.; Cousins, I. T.; Buck, R.; Korzeniowski, A. *Environ. Sci. Technol.* **2006**, *40*, 32–44.

(18) Moody, C. A.; Martin, J. W.; Kwan, W. C.; Muir, D. C. G.; Mabury, S. A. *Environ. Sci. Technol.* **2002**, *36*, 545–551.

(19) Hori, H.; Nagaoka, Y.; Murayma, M.; Kutsuna, S. *Environ. Sci. Technol.* **2008**, *42*, 7438–7443.

(20) Moody, C. A.; Kwan, W. C.; Martin, J. W.; Muir, D. C. G.; Mabury, S. A. *Anal. Chem.* **2001**, *73*, 2200–2206.

(21) Taniyasu, S.; Kannan, K.; Soc, M. K.; Gulkowska, A.; Sinclair, E.; Okazawa, T.; Yamashita, N. *J. Chromatogr. A* **2005**, *1093*, 89–97.

(22) Martin, J. W.; Smithwick, M. M.; Braune, B. M.; Hoekstra, P. F.; Muir, D. C. G.; Mabury, S. A. *Environ. Sci. Technol.* **2004**, *38*, 373–380.

(23) Bunn, C. W.; Howells, E. R. *Nature* **1954**, *174*, 549–551.

(24) Martin, J. W.; Kannan, K.; Berger, U.; Voogt, P. D.; Field, J.; Franklin, J.; Giesy, J. P.; Harner, T.; Muir, D. C. G.; Scott, B.; Kaiser, M.; Järnberg, U.; Jones, K. C.; Mabury, S. A.; Schroeder, H.; Simcik, M.; Sottani, C.; Bavel, B. V.; Kärrman, A.; Lindström, G.; Leeuwen, S. V. *Environ. Sci. Technol.* **2004**, *38*, 248A–255A.

(25) Voogt, P. d.; Sáez, M. *Trend. Anal. Chem.* **2006**, *25*, 326–342.

(26) Arsenault, G.; Chittim, B.; McAlees, A.; McCrindle, R.; Potter, D.; Tashiro, C.; Yeo, B. *Rapid Commun. Mass Spectrom.* **2007**, *21*, 929–936.

(27) Taniyasu, S.; Kannan, K.; Yeung, L. W. Y.; Kwok, K. Y.; Lam, P. K. S.; Yamashita, N. *Anal. Chim. Acta* **2008**, *619*, 221–230.

(28) Arsenault, G.; McAlees, A.; McCrindle, R.; Riddell, N. *Rapid Commun. Mass Spectrom.* **2007**, *21*, 3803–3814.

(29) Kissa, E. *J. Fluorine Chem.* **1994**, *66*, 5–6.

(30) Kudo, N.; Kawashima, Y. *J. Toxicol. Sci.* **2003**, *28*, 49–57.

(31) Conder, J.; Hoke, R.; Wolf, W. D.; Russell, M.; Buck, R. *Environ. Sci. Technol.* **2008**, *42*, 995–1003.

(32) Helgaker, T.; Jaszunski, M.; Ruud, K. *Chem. Rev.* **1999**, *99*, 293–352.

(33) Ribeiro, A. A. *J. Magn. Reson.* **1995**, *117*, 257–261.

(34) John, P. *Nature* **1968**, *217*, 1050–1051.

(35) Weigert, F. J.; Karel, K. J. *J. Fluorine Chem.* **1987**, *37*, 125–148.

(36) Taves, D. *Nature* **1966**, *211*, 192–193.

(37) Kimber, B. J.; Feeney, J.; Roberts, G. C. K.; Birdsall, B.; Griffiths, D. V.; Burcen, A. S. V. *Nature* **1978**, *271*, 184–185.

(38) Cornelissen, G.; VanNoort, P. C. M.; Nachtegaal, G.; Kentgens, A. P. M. *Environ. Sci. Technol.* **2000**, *34*, 645–649.

(39) Arsenault, G.; Chittim, B.; Gu, J.; McAlees, A.; McCrindle, R.; Robertson, V. *Chemosphere* **2008**, *73*, S53–S59.

(40) Arsenault, G.; Chittim, B.; McAlees, A.; McCrindle, R.; Robertson, V.; Riddell, N.; Yeo, B. *Chemosphere* **2008**, *73*, 616–625.

(41) Ellis, D. A.; Denkenberger, K. A.; Burrow, T. E.; Mabury, S. A. *J. Phys. Chem. A* **2004**, *108*, 10099–10106.

(42) Ilayaraja, N.; Manivel, A.; Velayutham, D.; Noel, M. *J. Appl. Electrochem.* **2008**, *38*, 175–186.

(43) Gramstad, T.; Haszeldine, R. N. *J. Chem. Soc.* **1957**, 2640–2645.

(44) Torres, F. J.; Ochoa-Herrera, V.; Blowers, P.; Sierra-Alvarez, R. *Chemosphere* **2009**, *76*, 1143–1149.

(45) Prakash, S. G. K.; Rasul, G.; Burrichter, A.; Laali, K. K.; Olah, G. A. *J. Org. Chem.* **1996**, *61*, 9253–9258.

(46) Ribeiro, A. A. *Magn. Reson. Chem.* **1997**, *35*, 215–221.

(47) Wiberg, K. B.; Hammer, J. D.; Zilm, K. W.; Cheeseman, J. R.; Keith, T. A. *J. Phys. Chem. A* **1998**, *102*, 8766–8773.

(48) Zhang, X.; Lerner, M. M. *Phys. Chem. Chem. Phys.* **1999**, *1*, 5065–5069.

(49) Fukaya, H.; Ono, T. *J. Comput. Chem.* **2003**, *25*, 51–60.

(50) Harding, M. E.; Lenhart, M.; Auer, A. A.; Gauss, J. *J. Chem. Phys.* **2008**, *128*, 244111-1–244111-10.

(51) Williams, D. E.; Peters, M. B.; Wang, B.; Merz Jr, K. M. *J. Phys. Chem. A* **2008**, *112*, 8829–8838.

(52) Liu, P.; Goddard, J. D.; Arsenault, G.; Gu, J.; McAlees, A.; McCrindle, R.; Robertson, V. *Chemosphere* **2007**, *69*, 1213–1220.

(53) Frisch, M. J.; Trucks, G. W.; Schlegel, H. B.; Scuseria, G. E.; Robb, M. A.; Cheeseman, J. R.; Montgomery, J. A., Jr.; Vreven, T.; Kudin, K. N.; Burant, J. C.; Millam, J. M.; Iyengar, S. S.; Tomasi, J.; Barone, V.; Mennucci, B.; Cossi, M.; Scalmani, G.; Rega, N.; Petersson, G. A.; Nakatsuji, H.; Hada, M.; Ehara, M.; Toyota, K.; Fukuda, R.; Hasegawa, J.; Ishida, M.; Nakajima, T.; Honda, Y.; Kitao, O.; Nakai, H.; Klene, M.; Li, X.; Knox, J. E.; Hratchian, H. P.; Cross, J. B.; Bakken, V.; Adamo, C.; Jaramillo, J.; Gomperts, R.; Stratmann, R. E.; Yazyev, O.; Austin, A. J.; Cammi, R.; Pomelli, C.; Ochterski, J. W.; Ayala, P. Y.; Morokuma, K.; Voth, G. A.; Salvador, P.; Dannenberg, J. J.; Zakrzewski, V. G.; Dapprich, S.; Daniels, A. D.; Strain, M. C.; Farkas, O.; Malick, D. K.; Rabuck, A. D.; Raghavachari, K.; Foresman, J. B.; Ortiz, J. V.; Cui, Q.; Baboul, A. G.; Clifford, S.; Cioslowski, J.; Stefanov, B. B.; Liu, G.; Liashenko, A.; Piskorz, P.; Komaromi, I.; Martin, R. L.; Fox, D. J.; Keith, T.; Al-Laham, M. A.; Peng, C. Y.; Nanayakkara, A.; Challacombe, M.; Gill, P. M. W.; Johnson, B.; Chen, W.; Wong, M. W.; Gonzalez, C.; Pople, J. A. *Gaussian 03*, revision C.02; Gaussian, Inc.: Wallingford, CT, 2004.

(54) Glendening, E. D.; Reed, A. E.; Carpenter, J. E.; Weinhold, F. *NBO*, Version 3.1; Institute of Theoretical Chemistry, University of Wisconsin, Madison, Wisconsin, 1988.

(55) Dixon, D. A. *J. Phys. Chem.* **1992**, *96*, 5331–5341.

(56) Knochenhauer, G.; Reiche, J.; Brehmer, L.; Barberka, T.; Woolley, M.; Tredgold, R.; Hodge, P. J. *Chem. Soc., Chem. Commun.* **1995**, 1619–1620.

(57) Albinsson, B.; Michl, J. *J. Am. Soc. Chem.* **1995**, *117*, 6378–6379.

(58) Jang, S. S.; Blanco, M.; Goddard, W. A., III; Caldwell, G.; Ross, R. B. *Macromolecules* **2003**, *36*, 5331–5341.

(59) Erkoc, S.; Erkoc, F. *J. Mol. Struct.: THEOCHEM* **2001**, *549*, 289–293.

(60) Ellis, D. A.; Denkenberger, K. A.; Burrow, T. E.; Mabury, S. A. *J. Phys. Chem. A* **2004**, *108*, 10099–10106.

(61) Dixon, D. A. *J. Phys. Chem.* **1992**, *96*, 3698–3701.

JP9078037